

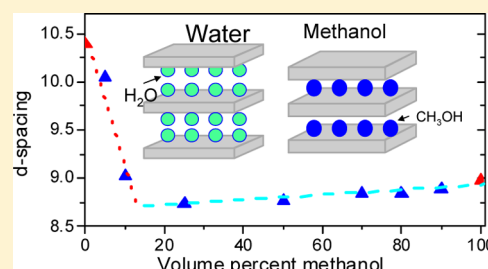
# Selective Intercalation of Graphite Oxide by Methanol in Water/Methanol Mixtures

Shujie You,<sup>†</sup> Junchun Yu,<sup>†</sup> Bertil Sundqvist,<sup>†</sup> L. A. Belyaeva,<sup>‡</sup> Natalya V. Avramenko,<sup>‡</sup> Mikhail V. Korobov,<sup>‡</sup> and Alexandr V. Talyzin<sup>\*,†</sup>

<sup>†</sup>Department of Physics, Umeå University, S-90187 Umeå, Sweden

<sup>‡</sup>Department of Chemistry, Moscow State University, Moscow 119991, Russia

**ABSTRACT:** Graphite oxide is selectively intercalated by methanol when exposed to liquid water/methanol mixtures with methanol fraction in the range 20–100%. Insertion of water into the GO structure occurs only when the content of water in the mixture with methanol is increased up to 90%. This conclusion is confirmed by both ambient temperature XRD data and specific temperature variations of the GO structure due to insertion/deinsertion of an additional methanol monolayer observed upon cooling/heating. The composition of GO–methanol solvate phases was determined for both low temperature and ambient temperature phases. Understanding of graphite oxide structural properties in binary water/methanol mixtures is important for understanding the unusual permeation properties of graphene oxide membranes for water and alcohols. It is suggested that graphite oxide prepared by Brodie's method can be used for purification of water using selective extraction of methanol from water/alcohol mixtures.



## 1. INTRODUCTION

Graphite oxide (GO) is a nonstoichiometric material with layered structure obtained by strong oxidation of graphite.<sup>1–3</sup> Oxidation results in an increase of the interlayer spacing up to ~6.5 Å and transformation of hydrophobic graphite into hydrophilic graphite oxide.<sup>4,5</sup> GO has attracted lots of research interest recently due to the possibility to disperse it as single sheets in solution, thus producing graphene oxide.<sup>6–12</sup> Graphene oxide can then be deposited as a thin film, a paper-like material, or a solid membrane.<sup>13–16</sup> Both graphene oxide and graphite oxide can easily be reduced back to graphene or graphite, e.g., by chemical or heat treatment.<sup>17–20</sup> Another unique property of GO is its ability to get intercalated (to solvate or to swell) by polar solvents when exposed to vapor or immersed in liquid solvent.<sup>4,5,21,22</sup> The main feature of GO solvation is a significant lattice expansion due to insertion of solvent between oxidized graphene layers.

The unique properties of GO have recently been suggested for some unusual applications, e.g., for fabrication of supercapacitors using laser-induced reductive patterning<sup>23</sup> or as a material for membranes which are permeable by water but not by ethanol or other polar solvents.<sup>24</sup> Separation of alcohols from water, suggested as application for such membranes, should be connected to specific structural properties of GO caused by hydration/solvation in water/alcohol mixtures. However, studies of GO hydration/solvation were so far limited to pure solvents and need to be extended to binary solvents.

Our recent experiments with graphite oxide immersed into excess of various liquid solvents showed an unusual phase transformation related to insertion/deinsertion of solvent into

the GO structure, and these transformations are strongly different in water compared to alcohols.<sup>25,26</sup> Insertion of additional solvent from a liquid medium into the GO structure occurs upon either cooling at ambient pressure or pressure increase at ambient temperature.<sup>25,27–31</sup> For all tested solvents except water (methanol, ethanol, acetone, dimethylformamide (DMF)) we observed phase transitions into low temperature (or high pressure) phases with a stepwise increase of the interlayer distance which correlates to intercalation of an additional monolayer of solvent molecules.<sup>26,30,32</sup> The pressure/temperature point of phase transition observed for GO immersed in these solvents does not correlate with the solidification point of the solvent.<sup>30</sup>

GO in excess of water shows a quite different hydration/dehydration behavior upon both temperature and pressure variations, characterized by an absence of clear steps correlated with insertion of solvent monolayers.<sup>25,27</sup> Cooling of GO/water samples results first in a gradual expansion of the interlayer spacing with a stepwise contraction at the freezing point of water.<sup>25</sup> It should be noted that the phase transitions related to insertion/deinsertion of solvent described above appeared to be strongly dependent on the particular method of GO synthesis, and most of the results described above were obtained for Brodie graphite oxide (B-GO).<sup>33</sup>

Here we present the results of a structural study performed on Brodie graphite oxide (B-GO) immersed in water/methanol mixtures of various compositions and performed over a broad

**Received:** December 26, 2012

**Revised:** January 9, 2013

**Published:** January 9, 2013

temperature interval. Selective intercalation of methanol from water–methanol mixtures is revealed in a certain composition range.

## 2. EXPERIMENTAL SECTION

The GO sample was prepared by Brodie's method from natural flaky graphite (99.98 wt % C; Graphitwerk Kropfmühl AG, Germany) with a final composition  $\text{CO}_{0.38}\text{H}_{0.12}$  (C:O atomic ratio  $\sim 2.63$ ) according to elemental analysis. Some XRD patterns recorded at ambient temperature were recorded using a conventional diffractometer with  $\lambda = 1.542$  nm. In-situ synchrotron radiation XRD cooling experiments (from room temperature down to about 150 K) were performed at the Max-Lab III beamline I711, Sweden. X-ray diffraction images were collected from powder samples loaded in glass capillaries with excess amounts of solvent using the transmission geometry. Temperature was controlled by an Oxford Cryosystems CryoStream 700+ cooler and decreased/increased in steps of 3–10 K. The radiation wavelength (1.0090 Å) was calibrated using a  $\text{LaB}_6$  standard. Fit2D software was used to integrate the diffraction images into diffraction patterns. Differential scanning calorimetry (DSC) was used to evaluate the enthalpy of the phase transformations. Graphite oxide powder and an excess amount of solvent (e.g., 2.0 mg of GO in 12.7 mg of methanol) were loaded into sealed aluminum sample capsules of ca. 50  $\mu\text{L}$  volume. The temperature was programmed to change at a 10 K/min rate on both cooling and heating. The samples were first cooled from room temperature to  $\sim 213$  K and then heated up.

Experiments performed with DCS below the freezing temperature of methanol were used to determine the composition of GO/methanol solvate. The main principle of the method is described in detail elsewhere.<sup>35</sup> In brief, the sample of GO with excess of liquid methanol is cooled down to the temperatures of solvate formation, then further cooled below the freezing point of the solvent, and upscanned. The endothermic peak due to methanol melting provides information about the amount of excess solvent, which was not incorporated into the GO solvate. The amount of solvent intercalated into GO can be calculated as the difference between total solvent mass known after loading and excess solvent mass calculated as described above.

If the amount of methanol was less than necessary for complete formation of the L-solvate, no melting of free methanol was observed. At low temperatures both L- and A-solvates were present in the system. The peak corresponding to the formation/decomposition of L-solvate in this case was lower than for the samples with the excess of methanol. The composition of A-solvate was calculated from the decrease of this latter peak.

Experiments that demonstrated a change of concentration after filtration of methanol/water liquid through the GO powder were performed using a Whatman 25 mm diameter alumina filter and filter holder; the powder of GO (typical amount 250 or 300 mg) was spread over the surface of the filter, making a film of about 1 mm in thickness (after wetting with a few drops of methanol and drying procedure). The concentration of methanol was performed using a portable densitometer (Densito 30PX, Mettler Toledo) with a precision of measurements of 0.1% (volumetric).

## 3. RESULTS AND DISCUSSION

Graphite oxide prepared by Brodie's method (B-GO) and immersed in excess of liquid methanol/water mixtures was first studied at ambient temperature. The hydration/solvation can be monitored using X-ray diffraction which provides information about the increase/decrease of the separation between graphene oxide layers caused by insertion/deinsertion of solvent from the liquid. At ambient conditions the saturated hydration/solvation is achieved within minutes upon immersion of samples into liquid media and results in immediate intercalation and lattice expansion. The interlayer separation of GO can be directly evaluated from the  $d$ -spacing obtained from the (001) reflection (see Figure 1).

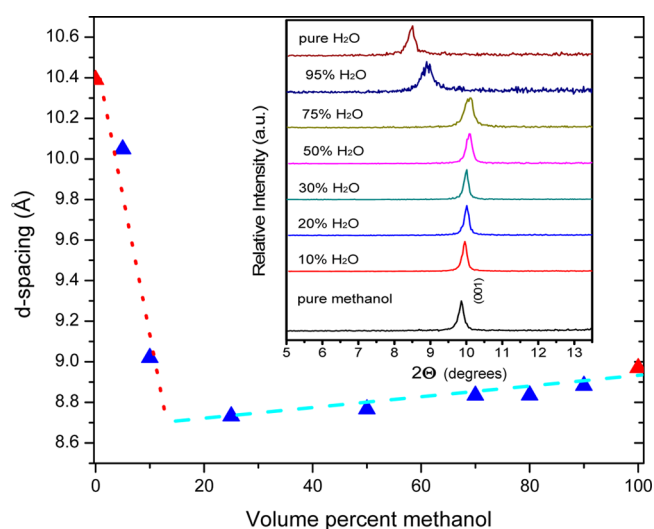


**Figure 1.** Interlayer distance ( $d$ -spacing calculated from the (001) reflection) of B-GO immersed in binary water/methanol mixtures of various compositions. Inset shows XRD patterns in the region of the (001) reflection.

The sample of B-GO shows significantly different interlayer distances when intercalated by water and methanol. At ambient temperature the  $d(001)$  spacing for GO in water is found as 10.39 Å while immersion of B-GO in liquid methanol yielded significantly smaller value (8.97 Å). Experiments with GO immersed in water/methanol mixtures of various compositions revealed rather interesting phenomena. Figure 1 demonstrates that  $d(001)$  of B-GO remains almost the same for methanol concentrations in the 20–100% range in binary mixtures with water and even becomes slightly smaller with increasing water content. An increase of the interlayer distance of B-GO was observed only for mixtures with water content 90% and higher.

The data shown in Figure 1 allow the following interpretation: methanol is selectively intercalated into the B-GO structure from water/methanol binary liquid media containing 20–80% methanol. For methanol concentrations of  $\sim 15\%$  and lower, GO is intercalated by both water and methanol. To our knowledge, this effect was not reported for graphite oxides previously and could possibly be used e.g. for water purification or extraction of methanol from water mixtures.

Selective intercalation of B-GO by methanol when immersed into water/methanol binary solvent with methanol concentrations in the range 20–100% was also confirmed by XRD experiments performed at low temperatures. Graphite oxide is

known to show rather different structural modifications upon cooling when immersed in liquid water and methanol media.<sup>25,30</sup> However, no structural data have so far been reported for GO immersed in water/methanol mixtures. Water solidifies at much higher temperature than methanol, thus providing a much narrower range of liquid phase existence. The presence of liquid solvent is crucial for intercalation of GO with various solvents. As was shown in our earlier study performed with GO powder immersed in pure water, cooling the system results in “pseudo-negative” thermal expansion: the *d*-spacing calculated from the (001) peak position gradually increases when temperature is lowered down to the point of ice formation. When water freezes, the interlayer distance shrinks by  $\sim 2$  Å, the sharp steplike decrease corresponding to deinsertion of one water monolayer.<sup>25</sup>

The B-GO immersed in pure methanol shows a rather distinct behavior upon cooling: a sharp phase transition due to insertion of an additional methanol monolayer was found at 253–254 K, but no change of structure upon further cooling down to 140 K and no structural change correlated with the solidification point of methanol.<sup>30</sup>

Therefore, if the GO structure is selectively intercalated only by methanol, it could be expected that a phase transition similar to the one observed at low temperatures for GO in pure methanol will also be found for water/methanol mixtures with 20–100% methanol.

Results from cooling experiments performed with B-GO samples immersed in water/methanol liquid media with various compositions are summarized in Figures 2 and 3. The first

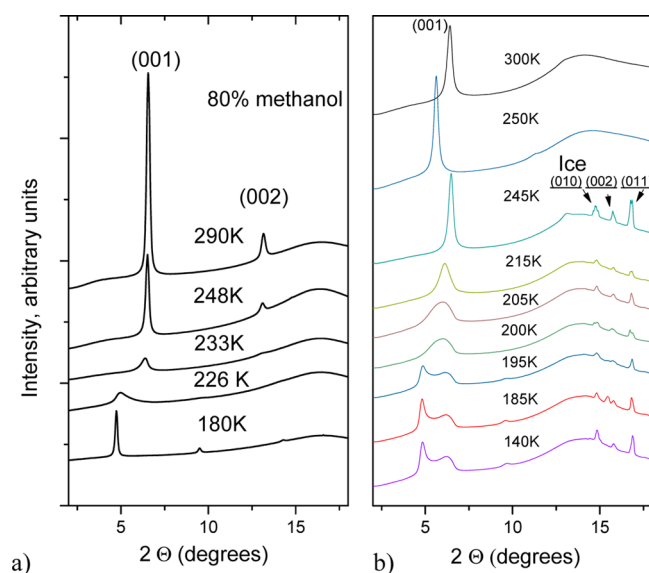


**Figure 2.** XRD patterns recorded for B-GO powder samples immersed in excess water/methanol solvents of the following compositions: (a) 80% methanol; (b) 10% methanol. Indexing is shown for B-GO reflections and in (b) for reflections from ice (underlined symbols).

experiments were performed with liquid media containing 90% and 80% of methanol. Both experiments exhibited results very similar to experiments with 100% methanol solvent: a phase transition due to insertion of an additional methanol monolayer and no significant variations of the interlayer distance at higher and lower temperatures. Figure 3 shows that one and the same GO solvated structure is formed with 100%, 80%, and 50% methanol solvent at low temperatures. The phase transition

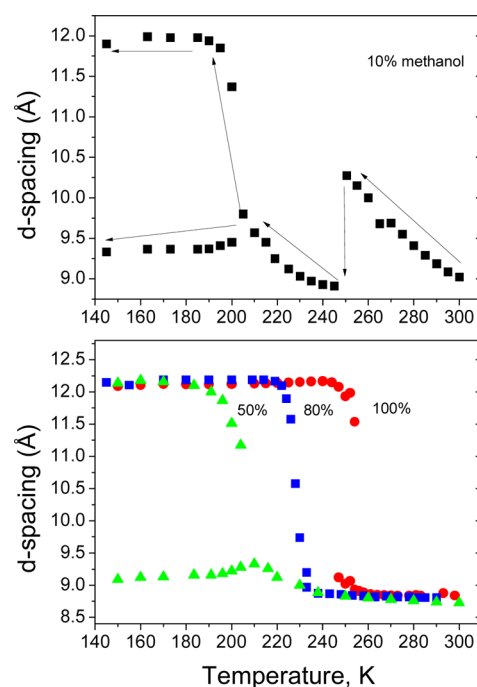


**Figure 3.** Temperature dependence of *d*(001) for GO powders immersed in excess of water/methanol mixtures, recorded upon cooling: (a) 10% methanol; (b) 50%, 80%, and 100% methanol.

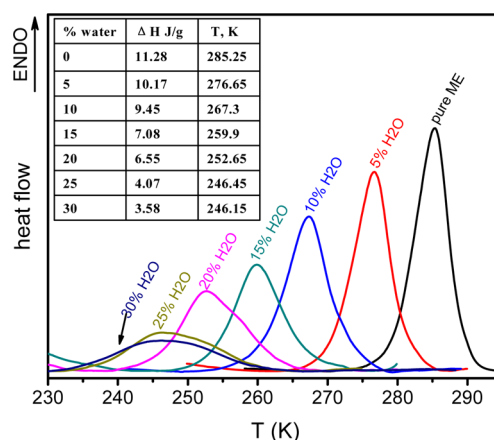


**Figure 4.** Endothermic peaks due to the phase transition between two solvates of GO (deinsertion of a solvent monolayer) in excess of water/methanol solvent as a function of volumetric % of water in the mixture; the data were recorded upon heating of precooled samples and rescaled to the same amount of graphite oxide. Inset shows table with numeric data for the enthalpy of the phase transition and the phase transition temperature.<sup>34</sup>

point is shifted to lower temperatures when the concentration of water in the water/methanol mixture is increased.

The phase transition between two solvate phases of B-GO in pure methanol can also be detected by DSC, and the enthalpy of transition was determined as 11.45 J/g.<sup>30</sup> For water/methanol mixtures this phase transition is still observed for a certain range of compositions. Figure 4 shows endothermic peaks due to deinsertion of solvent from the GO structure observed for samples cooled down to the low-temperature phase formation point and recorded upon heating back to room temperature. The endothermic effect observed for GO in Figure 4 is found to become broader and to shift to lower



temperatures and the enthalpy of transition decreased linearly with concentration when water was added to methanol. Assuming that the composition of the GO solvates is the same, the shift to lower temperatures is caused by the decrease of the thermodynamic activity of methanol in the methanol/water mixture compared to the case of pure methanol. The decrease of the enthalpy of transition in turn is explained by the partial enthalpy of mixing methanol with water.

XRD experiments with B-GO immersed in water rich (10% methanol) liquid media showed rather different results and more complicated structural transformations (Figure 3). In agreement with the trend shown in Figure 1, the temperature dependence of the (001) peak position for B-GO immersed in 10% methanol solvent showed features qualitatively similar to the dependence observed for pure water. However, the “pseudo-negative” thermal expansion of B-GO lattice appeared to be much more pronounced. The interlayer distance increased by about 1.5 Å down to the temperature of ice formation. At around 250 K a sharp steplike decrease of the interlayer spacing of B-GO was observed. As expected, this sharp change correlates with the point of ice formation, as evidenced by the reflections from ice found in patterns recorded below 250 K (Figure 2). However, some structural transformations were found also at lower temperatures.

As shown in Figure 3, the interlayer distance of the graphite oxide structure started to increase again below 245 K and around 205 K a second strong anomaly occurs. Below 205 K two (001) reflections are found. The difference between the *d*-spacings of these two (001) peaks corresponds to insertion of one additional methanol monolayer. Quite surprisingly, this anomaly looks almost the same as the phase transition between the A-phase and the L-phase in methanol-rich liquid, although the transformation is only partial and the peak from the low temperature phase is rather broad.

When the concentration of water was increased to 50% the partial phase transition into an expanded phase was also observed: for temperatures below 210 K two peaks were observed for the (001) reflection. However, no “negative thermal expansion” upon cooling and no effects at the point of ice formation (around 238 K) could be found. The sample shows a phase transition similar to that of GO in pure methanol except only for part of the material.

The results obtained for a concentration of 10% methanol in water/methanol mixtures can be explained by fractional crystallization of the water–methanol binary solvent which occurs according to the well-known phase diagram of this system. When the temperature of the system is lowered, B-GO in 10% methanol solution is intercalated mostly by water and the temperature dependence shows features typical for pure water, most importantly deinsertion of a water monolayer from the GO structure at the point of ice formation. However, crystallization of all the liquid does not occur at a single temperature (unlike pure water). As the crystallization of the water–methanol mixture proceeds, the liquid phase becomes richer in methanol while the melting point of this mixture becomes progressively lower. Therefore, a liquid phase is still present in the system even below the temperature point of ice formation (detected by XRD) while the GO structure has released one water monolayer and is capable to accommodate more solvent. At a certain temperature the methanol is intercalated into the GO structure and the lattice expands as shown in Figure 3. However, it is likely that water ice is blocking the access of liquid to some GO grains. As a result, the

phase transition is not complete and only a fraction of the sample is transformed into the L-phase. A very broad peak from the (001) reflection of the L-phase also indicates a possible interstratification of layers intercalated by water and methanol in different proportions.

The data presented above suggest that methanol can be selectively intercalated into the GO structure from liquid water/methanol mixtures in a certain concentration range. This effect can possibly be useful for extracting methanol from mixtures with water. Quantitative evaluation of the GO solvate phase composition is required for practical applications but no related data could be found in the literature. Therefore, an evaluation of the composition of the solvate phases of GO was performed by DSC experiments using GO samples loaded with excess amounts of methanol as described elsewhere<sup>35</sup> (see also Experimental Section). The results of these experiments are presented in Table 1. The mass ratio of methanol to GO was

**Table 1. Composition of GO–Methanol Solvates Determined from DSC Experiments**

phase	<i>N</i> <sup>a</sup>	mass ratio <sup>b</sup>	mol/g of GO <sup>c</sup>	molar ratio <sup>d</sup>
L	9	0.55 ± 0.4	0.017 ± 0.04	0.32 ± 0.08
A	7	0.28 ± 0.07	0.009 ± 0.02	0.16 ± 0.04

<sup>a</sup>Number of samples. <sup>b</sup>Mass ratio, solvent to GO. <sup>c</sup>Moles per gram of GO in the solvate. <sup>d</sup>Molar ratio solvent to molecular unit of GO calculated according to elemental composition CO<sub>0.38</sub>H<sub>0.12</sub>.

determined as 0.55 for the low-temperature phase. Considering the composition of the sample provided by the formula CO<sub>0.38</sub>H<sub>0.12</sub>, one can estimate that 0.64 methanol molecules per carbon ring is intercalated into the low-temperature solvate phase.

The composition of the L solvate determined here is consistent with two-layer intercalation of the GO structure, considering that the effective diameter of a methanol molecule is about 4.2 Å (as a comparison the diameter of a carbon hexagon is about 2.85 Å). The composition of the ambient temperature solvate phase was determined as 0.32 molecules of methanol per carbon hexagon ring (approximately 1 methanol molecule per 3 carbon rings), and according to our XRD data this corresponds to one methanol monolayer.

The results presented in previous section demonstrate the ability of B-GO powder to be selectively intercalated by methanol when exposed to water/methanol liquid media in the concentration range of 20–80% methanol. This conclusion is confirmed by both ambient temperature XRD data and by specific temperature variations of the GO structure due to insertion/deinsertion of additional methanol monolayers observed upon cooling/heating. One of the obvious applications of this effect is the extraction of methanol from methanol/water mixtures. A remarkable feature of the intercalation of methanol (and most other polar solvents) into the GO structure is that it is completely reversible. As soon as the powder is taken out of the solution and the methanol evaporates from the sample, the interlayer distance of the GO decreases back to ~6.5 Å, thus demonstrating the release of intercalated methanol. Extraction of methanol from mixtures with water can then be achieved by immersing GO powder into the binary solvent, followed by withdrawal of the powder saturated with methanol and evaporation of solvent from powder. This cycle can be repeated an infinite number of times as we observed no traces of sample degradation after several

cycles of immersion/drying the powder with methanol or water.

A simple experiment was performed in order to demonstrate the feasibility of using B-GO for selective absorption of methanol from methanol/water mixtures. Powder of B-GO (250–300 mg) was placed on the top of an alumina filter, slightly wetted with methanol to spread the powder homogeneously, and dried. The powder/filter sample was enclosed in a standard filter holder, thus making a very simple prototype of a B-GO filtration device. 3 mL of methanol/water solution with known concentration (in the range 30–90% of methanol) was passed through the filter over a period of about 1 min using a syringe, and the concentration of methanol was measured again. Then the powder was dried and a new portion of solution passed through. All experiments demonstrated a decrease of the methanol concentration in the filtrated liquid by 1–2.4%. The maximum change in methanol concentration was achieved when powder was dried overnight before filtering and more homogeneously distributed over the filter. If the filtered solution was passed through the powder immediately after the first filtration (without powder drying), no change of concentration was observed. Also, no change in concentration was observed for water-rich solution (13% of methanol) in agreement with the XRD data shown in Figure 1. The maximum change of liquid phase composition observed in our experiments corresponds to absorption of about 0.24 (mass ratio of absorbed solvent to mass of GO) by simply passing of methanol through the powder. This value is in rather good agreement with the composition of the A-phase of B-GO (see Table 1). Absorption of methanol from a binary liquid mixture was also confirmed using an additional DSC test. In this experiment 4.1 mg of powder was immersed in 11 mg of methanol/water mixture of known concentration (25.3 wt %). The change in composition of the liquid phase can be approximately evaluated using the change of melting point which becomes 3.1 K higher. The increase of the melting point is consistent with the expected intercalation of some methanol into the B-GO structure which makes the liquid phase richer in water.

It should be noted here that this effect is likely to be limited only to graphite oxide produced by Brodie's method. According to our earlier studies, the graphite oxide prepared by Hummers' method (H-GO) is solvated rather differently compared to B-GO. The Hummers method involves a more complex combination of chemicals which results in an oxidation product which is less crystalline, shows significantly different exfoliation temperature, and is more easily dispersed in water using sonication. A more detailed analysis of B-GO and H-GO properties and functionality can be found in our earlier study.<sup>33</sup> The H-GO shows an interlayer distance of 12.4 Å when immersed in water and 13.15 Å in liquid methanol at ambient temperature. It can be assumed that B-GO is intercalated by one methanol monolayer at ambient temperatures while H-GO is intercalated by at least two monolayers. It is convenient to use in the discussion two terms common in clay mineralogy: crystalline swelling (see e.g. ref 36), which corresponds to insertion by of certain number of solvent monolayers, and osmotic swelling (see example in ref 37), denoting insertion of liquid-state solvent by several monolayers simultaneously.

The H-GO shows similar osmotic swelling for both water and methanol. The unique property of B-GO is that only the insertion of water occurs by osmotic swelling, while insertion of all other (so far studied) polar solvents occurs as crystalline

swelling. Crystalline swelling of B-GO was observed in our previous studies not only for alcohols (methanol, ethanol, propanol<sup>26</sup>) but also for other polar solvents, e.g., acetone<sup>28</sup> and dimethylformamide.<sup>30</sup> Therefore, it can be anticipated that the effect of selective intercalation of B-GO is not only typical for methanol/water mixtures but also for other binary mixtures of water with polar solvents. It should be noted that a similar effect was previously reported for some clay minerals.<sup>38</sup>

It is interesting also to discuss possible implications of the results presented here for the properties of graphene oxide membranes. The results obtained here are valid for powder samples with typical flake sizes of a few micrometers. The membranes prepared by Nair et al.<sup>24</sup> are micrometers thick and consist of multiple graphene oxide layers. Therefore, the membranes can also be considered as graphite oxide but with "flake" sizes on the centimeter scale. It is unclear how flake size and geometry will influence structural modifications of the material in various liquid media. However, it can be suggested that the difference in hydration/solvation of the precursors H-GO and B-GO will also be reflected in the properties of membranes.

It should be noted that unusual permeation properties of water/alcohols have been found so far only for membranes prepared using graphite oxide synthesized by Hummers' method and only when exposed to vapors.<sup>24</sup> The results reported here were obtained for Brodie GO and can be directly applied only for membranes immersed in liquids. The H-GO is easily dispersed as single sheets in water using sonication, while dispersion of B-GO can be achieved only in slightly basic solutions. Thus, preparation of membranes should be possible also for B-GO material. However, it can be anticipated that membranes prepared from B-GO will exhibit different permeation properties. The structural study performed here allows us to suggest that for methanol concentrations in the 20–100% range in water/methanol mixtures graphite oxide will be selectively intercalated by methanol, thus making permeation of water through the membrane impossible.

In general, the properties of graphite oxide can be varied strongly using different degrees of oxidation and different synthesis methods and further modified by functionalization. Therefore, it can be expected that graphene (or graphite) oxide membranes with enormous variations of their permeation properties can be prepared in the future and optimized for specific applications, e.g., related to selective permeation of certain components of solvent mixtures.

## AUTHOR INFORMATION

### Corresponding Author

\*E-mail alexandr.talyzin@physics.umu.se.

### Notes

The authors declare no competing financial interest.

## ACKNOWLEDGMENTS

This work was financially supported by the Swedish Research Council, grants 621-2010-3732 and 621-2012-3654. A.T. thanks Ängpanneföreningens Forskingsstiftelse for financial support. L.A.B., N.V.A., and M.V.K. were supported by the RFBR grant 12-03-000653 and by the grant for Leading Scientific Schools in Russia. We thank Dr. Carsten Gundlach and Dr. Diana Thomas for the help with low-temperature XRD experiments performed at MAX-lab III, beamline I711.

## ■ REFERENCES

- (1) Brodie, B. C. *Ann. Chim. Phys.* **1860**, 59, 466–72.
- (2) Hummers, W. S.; Offeman, R. E. *J. Am. Chem. Soc.* **1958**, 80, 1339–1339.
- (3) Hofmann, U. F. A. *Ber. Deutsch. Chem. Ges.* **1930**, 63, 14.
- (4) Boehm, H. P.; Clauss, A.; Hofmann, U. *J. Chim. Phys. Phys.-Chim. Biol.* **1961**, 58, 141–147.
- (5) de Boer, J. B.; van Doorn, A. B. C. *Koninkl. Nederl. Akad. Wetenschappen, Ser. B* **1958**, 61, 242–252.
- (6) Szabo, T.; Hornok, V.; Schoonheydt, R. A.; Dekany, I. *Carbon* **2010**, 48, 1676–1680.
- (7) Szabo, T.; Tombacz, E.; Illes, E.; Dekany, I. *Carbon* **2006**, 44, 537–545.
- (8) Kim, J.; Cote, L. J.; Kim, F.; Yuan, W.; Shull, K. R.; Huang, J. *J. Am. Chem. Soc.* **2010**, 132, 8180–8186.
- (9) Li, D.; Muller, M. B.; Gilje, S.; Kaner, R. B.; Wallace, G. G. *Nat. Nanotechnol.* **2008**, 3, 101–105.
- (10) Stankovich, S.; Dikin, D. A.; Dommett, G. H. B.; Kohlhaas, K. M.; Zimney, E. J.; Stach, E. A.; Piner, R. D.; Nguyen, S. T.; Ruoff, R. S. *Nature* **2006**, 442, 282–286.
- (11) Paredes, J. I.; Villar-Rodil, S.; Martínez-Alonso, A.; Tascón, J. M. D. *Langmuir* **2008**, 24, 10560–10564.
- (12) Gilje, S.; Han, S.; Wang, M.; Wang, K. L.; Kaner, R. B. *Nano Lett.* **2007**, 7, 3394–3398.
- (13) Dikin, D. A.; Stankovich, S.; Zimney, E. J.; Piner, R. D.; Dommett, G. H. B.; Evmenenko, G.; Nguyen, S. T.; Ruoff, R. S. *Nature* **2007**, 448, 457–460.
- (14) Chen, C. M.; Yang, Y. G.; Wen, Y. F.; Yang, Q. H.; Wang, M. Z. *New Carbon Mater.* **2008**, 23, 345–350.
- (15) Chen, C. M.; Yang, Q. H.; Yang, Y. G.; Lv, W.; Wen, Y. F.; Hou, P. X.; Wang, M. Z.; Cheng, H. M. *Adv. Mater.* **2009**, 21, 3007–3011.
- (16) Eda, G.; Chhowalla, M. *Adv. Mater.* **2010**, 22, 2392–2415.
- (17) Schniepp, H. C.; Li, J. L.; McAllister, M. J.; Sai, H.; Herrera-Alonso, M.; Adamson, D. H.; Prud'homme, R. K.; Car, R.; Saville, D. A.; Aksay, I. A. *J. Phys. Chem. B* **2006**, 110, 8535–8539.
- (18) McAllister, M. J.; Li, J. L.; Adamson, D. H.; Schniepp, H. C.; Abdala, A. A.; Liu, J.; Herrera-Alonso, M.; Milius, D. L.; Car, R.; Prud'homme, R. K.; Aksay, I. A. *Chem. Mater.* **2007**, 19, 4396–4404.
- (19) Jeong, H.-K.; Lee, Y. P.; Jin, M. H.; Kim, E. S.; Bae, J. J.; Lee, Y. H. *Chem. Phys. Lett.* **2009**, 470, 255–258.
- (20) Talyzin, A. V.; Szabo, T.; Dekany, I.; Langenhorst, F.; Sokolov, P. S.; Solozhenko, V. L. *J. Phys. Chem. C* **2009**, 113, 11279–11284.
- (21) Buchsteiner, A.; Lerf, A.; Pieper, J. *J. Phys. Chem. B* **2006**, 110, 22328–22338.
- (22) Lerf, A.; Buchsteiner, A.; Pieper, J.; Schottl, S.; Dekany, I.; Szabo, T.; Boehm, H. P. *J. Phys. Chem. Solids* **2006**, 67, 1106–1110.
- (23) Gao, W.; Singh, N.; Song, L.; Liu, Z.; Reddy, A. L. M.; Ci, L. J.; Vajtai, R.; Zhang, Q.; Wei, B. Q.; Ajayan, P. M. *Nat. Nanotechnol.* **2011**, 6, 496–500.
- (24) Nair, R. R.; Wu, H. A.; Jayaram, P. N.; Grigorieva, I. V.; Geim, A. K. *Science* **2012**, 335, 442–444.
- (25) Talyzin, A. V.; Luzan, S. M.; Szabo, T.; Chernyshev, D.; Dmitriev, V. *Carbon* **2011**, 49, 1894–1899.
- (26) Talyzin, A. V.; Sundqvist, B.; Szabo, T.; Dekany, I.; Dmitriev, V. *J. Am. Chem. Soc.* **2009**, 131, 18445–18449.
- (27) Talyzin, A. V.; Solozhenko, V. L.; Kurakevych, O. O.; Szabo, T.; Dekany, I.; Kurnosov, A.; Dmitriev, V. *Angew. Chem., Int. Ed.* **2008**, 47, 8268–8271.
- (28) Talyzin, A. V.; Luzan, S. M. *J. Phys. Chem. C* **2010**, 114, 7004–7006.
- (29) Luzan, S. M.; Talyzin, A. V. *J. Phys. Chem. C* **2011**, 115, 24611–24614.
- (30) You, S.; Luzan, S. M.; Yu, J.; Sundqvist, B.; Talyzin, A. *J. Phys. Chem. Lett.* **2012**, 3, 812–817.
- (31) Talyzin, A. V.; Sundqvist, B.; Szabo, T.; Dmitriev, V. *J. Phys. Chem. Lett.* **2011**, 2, 309–313.
- (32) You, S.; Luzan, S.; Yu, J.; Sundqvist, B.; Talyzin, A. V. *J. Phys. Chem. Lett.* **2012**, 812–817.
- (33) You, S.; Luzan, S. M.; Szabo, T.; Talyzin, A. V. *Carbon* **2013**, 52, 171–180.
- (34) You, S.; Yu, J.; Sundqvist, B.; Talyzin, A. V. *Phys. Status Solidi B* **2012**, 249, 2568–2571.
- (35) Korobov, M. V.; Mirakyan, A. L.; Avramenko, N. V.; Olofsson, G.; Smith, A. L.; Ruoff, R. S. *J. Phys. Chem. B* **1999**, 103, 1339–1346.
- (36) Devineau, K.; Bihannic, I.; Michot, L.; Villieras, F.; Masrouri, F.; Cuisinier, O.; Fragneto, G.; Michau, N. *Appl. Clay Sci.* **2006**, 31, 76–84.
- (37) Amorim, C. L. G.; Lopes, R. T.; Barroso, R. C.; Queiroz, J. C.; Alves, D. B.; Perez, C. A.; Schelin, H. R. *Nucl. Instrum. Methods Phys. Res., Sect. A* **2007**, 580, 768–770.
- (38) Brindley, G. W.; Wiewiora, K.; Wiewiora, A. *Am. Mineral.* **1969**, 54, 1635–1644.